

# Etching of buried photoresist layers and its application to the formation of three-dimensional layered structures

T. Watanabe<sup>1</sup>, T. Sameshima<sup>1\*</sup>, M. Ide<sup>2</sup>

<sup>1</sup>Tokyo University of Agriculture and Technology, 2–24–16 Nakacho, Koganei, Tokyo 184–8588, Japan

<sup>2</sup>Citizen Watch Co. Ltd, 840 Shimotomi, Tokorozawa, Saitama 359–8511, Japan

Received: 22 January 2001/Accepted: 24 January 2001/Published online: 27 June 2001 – © Springer-Verlag 2001

**Abstract.** The fabrication of three-dimensional layered structures with 180-nm-thick TaO<sub>x</sub> top layers supported by 1.5- $\mu$ m-thick Mo pillars formed on a glass substrate is presented. The photoresist used for planarization was successfully removed through the TaO<sub>x</sub> layers using heat treatment at 270 °C with mixed vapors of ethyl alcohol and pure water at high pressure for 3 h. Vacancies underlying the TaO<sub>x</sub> layers were consequently formed. The possibility of rapid and lateral crystallization of amorphous silicon films was demonstrated when the silicon films formed on the TaO<sub>x</sub> overlaying the vacancy regions were irradiated using a frequency-doubled YAG laser at 250 mJ/cm<sup>2</sup>. Energy sensors using Cr/Al metal wires, with a high sensitivity of 0.07 mW/cm<sup>2</sup>, were also demonstrated using the present structure with vacancy regions for reduction of heat diffusion.

**PACS:** 85.85.+j; 81.65.Cf; 61.50.-f; 44.10.+i

Microstructure fabrication technologies of have been improving in the field of microelectromechanical systems (MEMS), such as integrated electric circuits, actuators and sensors [1–5]. The development of fabrication technologies has resulted in an unprecedented range of devices. Micro-vacant regions are used in three-dimensional thin-film layered structures, for example, micro-field emitters (MFE) [6] and digital micro-mirror displays (DMD) [7]. Thermal conductivity can be controlled in vertical as well as lateral directions by the distribution of micro-vacant regions. Calorimetric energy sensors become more sensitive by reduction of heat dissipation using air gaps [8]. Also, micro-vacancies have advantages for reducing the interconnecting delay in multilayered wiring for very large-scale integrated electronic circuits because they reduce the effective dielectric coefficient [8–12].

In this paper, we report on the etching of buried photoresist layers through overlaying insulating layers using heat treatment with high-pressure alcoholic vapor. Characterization and optimization of the etching behavior are presented

for the formation of micro-vacant regions. Three-dimensional layered structures with micro-vacant regions are applied to crystallization of silicon films and energy sensor fabrication for controlling thermal conductance.

## 1 Experimental procedure

The fabrication process steps for the three-dimensional structure are shown in Fig. 1. Molybdenum (Mo) pillars with

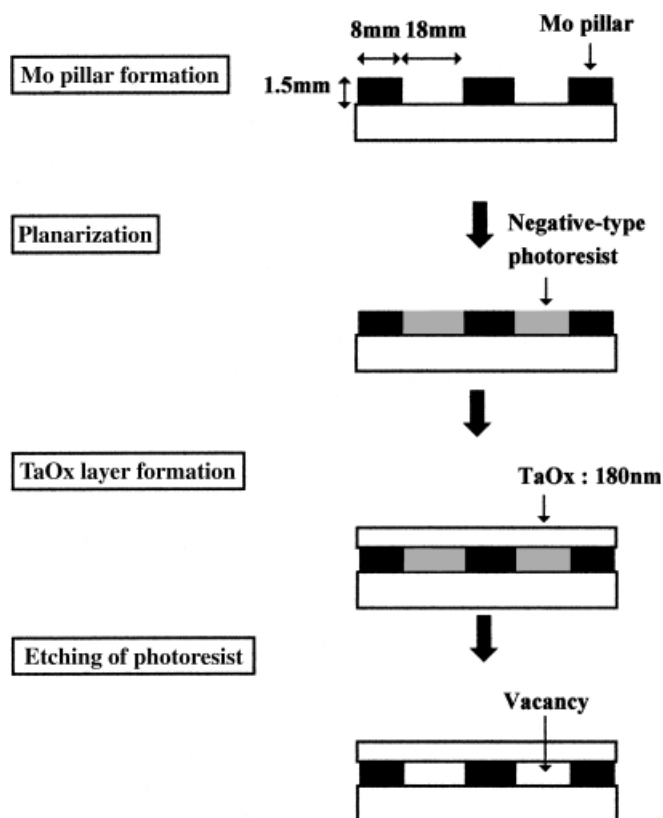


**Fig. 1.** Schematic process step of the present structure

\*Corresponding author.

(Fax: +42/388-7436, E-mail: tsamesim@cc.tuat.ac.jp)

a thickness of 1.5  $\mu\text{m}$  and a diameter of 8  $\mu\text{m}$  were formed on a glass substrate with a period of 26  $\mu\text{m}$  using sputtering and etching techniques. The negative-type photoresist was coated over the Mo pillars and substrate. Planarization of the photoresist was carried out by oxygen plasma treatment until the surfaces of photoresist and Mo pillars leveled off.  $\text{TaO}_x$  layers with a thickness of 180 nm were sputtered onto the top surface. The photoresist and Mo pillars were buried by the  $\text{TaO}_x$  layers. To remove the buried photoresist, heat treatment at 270  $^\circ\text{C}$  with ethyl alcohol and pure water vapor at a pressure of about  $3 \times 10^7$  Pa was carried out in a pressure-proof stainless chamber having a volume of 30  $\text{cm}^3$ . Optical transmissivity spectra in the ultraviolet region were measured in order to investigate etching behavior of the photoresist. Scanning electron microscopy (SEM) was also used in order to demonstrate the three-dimensional layered structure, including buried vacant regions by cross-sectional imaging.

The structure was applied to laser crystallization and calorimetric energy sensing. For laser crystallization, amorphous silicon films with a thickness of 70 nm were formed on top of the  $\text{TaO}_x$  layer at 200  $^\circ\text{C}$  by plasma-enhanced chemical vapor deposition after etching the photoresist. The amorphous silicon films were irradiated using a 5-ns-pulsed 532-nm frequency-doubled YAG laser at room temperature. Optical reflectivity spectra as well as Raman scattering spectra were measured in order to investigate the crystallization. For energy sensor application, a double metal layer consisting of a chromium layer with a thickness of 50 nm overlaying an aluminum layer with a thickness of 250 nm was formed on the  $\text{TaO}_x$  layer using thermal evaporation after photoresist etching. The Cr/Al wire patterns had a defined width of 20  $\mu\text{m}$  and a length of 250  $\mu\text{m}$  by etching. A voltage of 0.05 V was applied to the wires. The wire samples were illuminated with 1700 K-black body radiation in air at room temperature. The changes in resistivity of the wires caused by the illumination were measured using a Wheatstone bridge circuit.

## 2 Results and discussion

Before fabrication of the three-dimensional layered structures, the etching rate of photoresist was investigated using a single layer of photoresist coated on a single crystalline silicon wafer. Figure 2 shows the etching rate of the photoresist as a function of heating temperature when subjected to the vapor of pure ethyl alcohol as well as a mixed vapor of ethyl alcohol and pure water with a volume ratio of 19/1. The total amount of liquid was fixed 10  $\text{cm}^3$  in every case. The vapor pressure was  $3 \times 10^7$  Pa at 270  $^\circ\text{C}$ . The etching rate of the photoresist was confirmed by the reflective spectra in the visible region using an optical spectrophotometer. The photoresist was not etched at room temperature with those solutions. Following heat treatment with pure ethyl alcohol vapor, the etching rate increased from 0.2 to 0.4  $\mu\text{m}/\text{h}$  as the temperature increased from 100 to 270  $^\circ\text{C}$ . However, in the case of heat treatment with mixed vapor of ethyl alcohol and pure water, the etching rate increased from 0.5 to 1.9  $\mu\text{m}/\text{h}$  as the temperature increased from 100 to 270  $^\circ\text{C}$ . It is interesting to note that ethyl alcohol alone is not sufficient for etching the photoresist.  $\text{H}_2\text{O}$  vapor promotes the etching of photoresist under high pressures. When photoresist/Si samples were heated at 270  $^\circ\text{C}$  in  $3 \times 10^7$  Pa pure water vapor, the

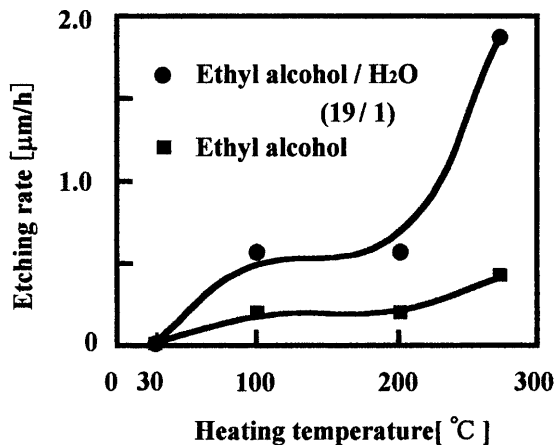


Fig. 2. Etching rate of photoresist as a function of heating temperature for a single layer of photoresist on a single crystalline silicon wafer at 270  $^\circ\text{C}$  with  $3 \times 10^7$  Pa in the cases of pure-ethyl alcohol vapor and mixed vapors of ethyl alcohol and  $\text{H}_2\text{O}$  with volume ratio of 19/1

photoresist became very glutinous. This indicates that  $\text{H}_2\text{O}$  vapor softens the photoresist and enhances the possibility of reaction and dissociation of photoresist with ethyl alcohol vapor.

The etching of photoresist buried by the  $\text{TaO}_x$  top layer was then carried out. Figure 3 shows transmissivity as a function of wavelength before and after heat treatment. Before heat treatment, the transmissivity was 0.2% at 308 nm, because of the large optical absorption of the photoresist. However, heat treatment at 270  $^\circ\text{C}$  for 3 h with  $3 \times 10^7$  Pa pure ethyl alcohol vapor increased the transmissivity to 3% at 308 nm. This means that etching of buried photoresist occurred with the ethyl alcohol vapor. Heat treatment with the mixed vapor of ethyl alcohol and pure water (19/1) further increased the transmissivity to 9% at 308 nm. Etching of the photoresist was then effectively achieved by the heat treatment. Figure 4 shows the cross-sectional SEM images of the  $\text{TaO}_x$  overlaying the Mo pillars on glass substrates before heat treatment (a) and after heat treatment with the mixed vapor of ethyl alcohol and pure water (b). The SEM image (b)

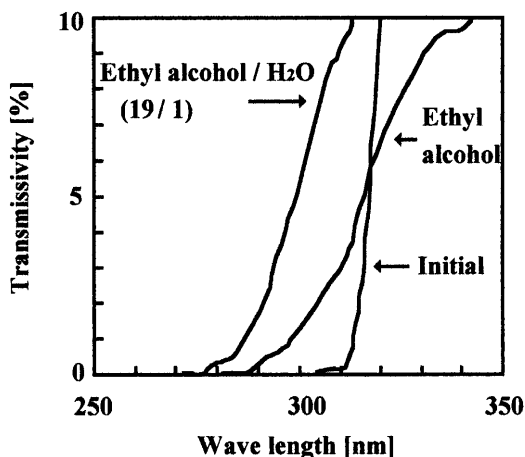
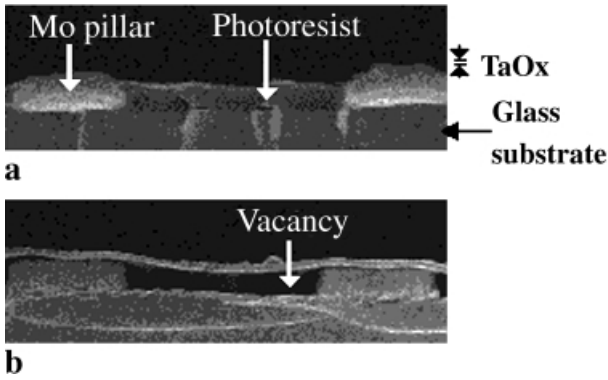


Fig. 3. Transmissivity in the ultra violet region before and after etching of a photoresist buried by a  $\text{TaO}_x$  top layer with heat treatment at 270  $^\circ\text{C}$  for 3 h with the vapor of pure-ethyl alcohol and mixed vapors of ethyl alcohol and  $\text{H}_2\text{O}$  with volume ratio of 19/1 at  $3 \times 10^7$  Pa



**Fig. 4a,b.** Cross-sectional SEM image **a** before heat treatment and **b** heat treatment at 270 °C for 3 h with  $3 \times 10^7$  Pa mixed vapors of ethyl alcohol and H<sub>2</sub>O with a volume ratio of 19/1

clearly shows the complete etching of the photoresist underlying the TaO<sub>x</sub> layer. No residual materials were observed in the vacancy regions. The TaO<sub>x</sub> layer and Mo pillars were not destroyed by the heat treatment. The mixed solution was effective for the etching of photoresist under the present conditions, although no holes were formed in the TaO<sub>x</sub> layers for etching of photoresist. We interpret the etching of the photoresist as being due to the gaseous ethyl alcohol and H<sub>2</sub>O being incorporated into the very narrow gaps ( $\sim$  nm) between the TaO<sub>x</sub> grains and into the underlying region during heat treatment, leading to dissociation of the photoresist. High-pressure H<sub>2</sub>O vapor softens the photoresist and enhances the etching rate of the photoresist by ethyl alcohol.

We used the structure containing the small vacancies for laser crystallization of amorphous silicon films. Figure 5 shows the Stokes Raman scattering spectra of the initial a-Si films and films irradiated by 5-ns-pulsed 532-nm frequency-doubled YAG laser radiation at 250 mJ/cm<sup>2</sup>, at points just above the Mo pillars and at the middle point above a vacancy region, as shown by the inset. The spectrum of initial a-Si films showed a broad peak around 480 cm<sup>-1</sup> due to the

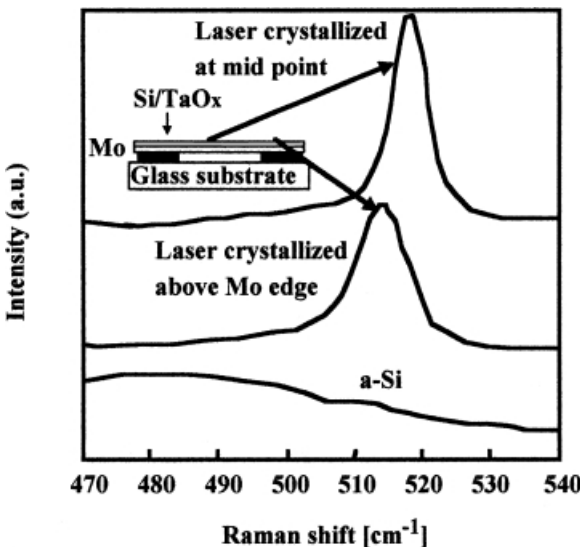


**Fig. 5.** Stokes Raman scattering spectra of an amorphous silicon film and films irradiated by pulsed laser at 250 mJ/cm<sup>2</sup> just above Mo pillars and middle point above air vacancies

amorphous TO phonon. After YAG laser heating, a sharp peak around 516 cm<sup>-1</sup>, associated with the transverse optical (TO) phonon of crystalline silicon, appeared in the spectrum of the silicon films just above the Mo pillars. That spectrum had a small broad peak in the wave number region below 516 cm<sup>-1</sup>. This means that the silicon films just above the Mo pillars were not crystallized completely because of high heat diffusivity of the Mo pillars (139 W/mK). However, the sharp peak of the crystalline TO phonon at 518 cm<sup>-1</sup> and no residual broad peak were observed in the spectrum of the silicon films at the middle point above a vacancy region. As the peak wave number of the single crystalline silicon wafer was 520.03 cm<sup>-1</sup> [13], there was a tensile stress in the crystallized silicon films on the TaO<sub>x</sub> films. The peak shift gave a film stress of  $4.0 \times 10^8$  Pa in the case of the middle region. Although the bandwidth just above the Mo pillars was 10.5 cm<sup>-1</sup>, it was 6 cm<sup>-1</sup> at the middle position of the vacancy region. The silicon films above the vacancy were effectively heated by laser irradiation and crystallized well because of the low thermal diffusivity of air ( $2.4 \times 10^{-2}$  W/mK). These results indicate the possibility of grain growth in the lateral direction according to the temperature gradient due to different effective thermal conductivities of Mo and air vacancies. Heat flow in the lateral direction to the Mo regions will occur and a temperature gradient will be generated. Spatial control of crystallization around Mo pillars would be possible.

Calorimetric energy sensors were fabricated using the present three-dimensional layered structure as shown by inset in Fig. 6. Figure 6 shows the changes in resistivity ( $(R_{\text{photo}} - R_{\text{dark}})/R_{\text{dark}}$ ) of Cr/Al wires at 0.1 s after initiation of illumination as a function of the intensity of the light source. The Cr/Al sensors were also fabricated directly on quartz substrates for comparison. The resistivity of the Cr/Al wires on the three-dimensional layered structure increased as the photo intensity increased. Because the detection limit of resistivity change was  $4 \times 10^{-6}$  at 0.1 s after the initiation of light illumination, the lower detection limit of photo intensity was

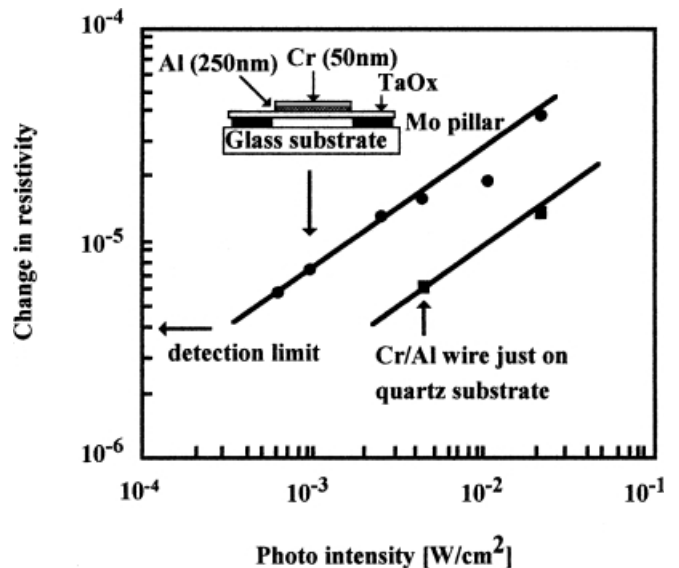


**Fig. 6.** Changes in resistivity of Cr/Al wires on the present structure and on a quartz substrate at 0.1 s after initiation of illumination as a function of the intensity of the light source

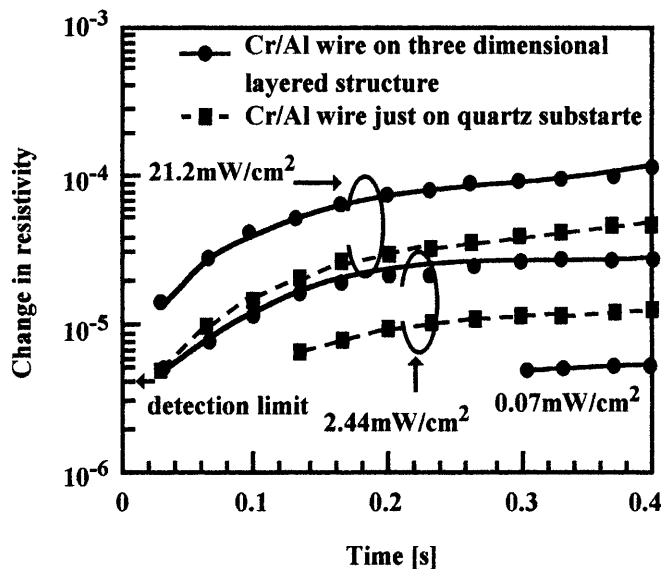


Fig. 7. Changes in resistivity of Cr/Al wires on present structure and on a quartz substrate as a function of time in the case of photo intensities of 0.07, 2.44 and 21.2 mW/cm<sup>2</sup>

estimated as 0.3 mW/cm<sup>2</sup> at 0.1 s. Vacancies in the three-dimensional layered structure effectively reduced the heat diffusivity so that the Cr/Al sensors became sensitive to illumination intensity. However, the lower limit was 2 mW/cm<sup>2</sup> at 0.1 s after initiation of illumination for the sensors fabricated directly on quartz substrates because of the high heat diffusivity of the quartz substrate (1.4 W/mK). Figure 7 shows changes in the resistivity as a function of time with different photo intensities of 0.07, 2.44 and 21.2 mW/cm<sup>2</sup>. The Cr/Al sensors on the three-dimensional layered structure containing vacancies on the glass substrate showed a slight change in resistivity at 0.3 s after initiation of illumination at 0.07 mW/cm<sup>2</sup>, which was at the lower detection limit in the present experimental system. Change in the resistivity was more quickly detected at 0.03 s when the sensor was illuminated at 2.44 mW/cm<sup>2</sup>. The resistivity change increased by 5 times at 0.4 s after illumination because of heating of Cr/Al sensors as shown in Fig. 7. The 1.5- $\mu$ m-thick vacancies had an important role in determining the effective heat resistivity in that time range. However, the sensors formed on the quartz substrate had a lower energy sensitivity. It took 0.14 s to observe a change in the resistivity of the sensor under illumination at 2.44 mW/cm<sup>2</sup>.

### 3 Summary

We have developed an etching process for buried photoresist layers on the surface of glass substrates using heat treatment with high-pressure alcoholic vapor to form small vacant regions. Photoresist was used for planarization of Mo pillars having a thickness of 1.5  $\mu$ m and a diameter of 8  $\mu$ m formed with a period of 26  $\mu$ m on glass substrates. After formation of TaO<sub>x</sub> layers with a thickness of 180 nm on the surfaces

of the photoresist and Mo pillars, samples were heated at 270 °C for 3 h with mixed vapors of ethyl alcohol and pure water vapor having a volume ratio of 19/1 at  $3 \times 10^7$  Pa. Observations using optical transmissivity spectra and cross-sectional SEM images revealed that the photoresist buried by the TaO<sub>x</sub> layers was removed and vacancies were formed beneath the TaO<sub>x</sub> layers. We interpret the etching of the photoresist as being due to the gaseous ethyl alcohol and H<sub>2</sub>O being incorporated into the very narrow gaps ( $\sim$  nm) between the TaO<sub>x</sub> grains and into the underlying region during heat treatment, and there reacting with and dissociating the photoresist. The pure water vapor promoted the etching rate of photoresist by softening the photoresist. Laser crystallization was demonstrated with the present structure. 70-nm-thick amorphous silicon films formed on the TaO<sub>x</sub> layer overlaying the vacancies were crystallized well by irradiation with a 5-ns pulsed 532-nm frequency-doubled YAG laser at 250 mJ/cm<sup>2</sup>, while films formed on the TaO<sub>x</sub> layer above the Mo pillars had residual amorphous regions after the laser irradiation because of the high heat diffusivity of the Mo pillars compared with that of the air vacancies. Heat diffusion is generated from the region above vacancies to the region above Mo pillars so that the grain growth in the lateral direction occurs. Calorimetric energy sensors were also demonstrated. The resistivity response was measured at an illumination of 1700 K black body light at 0.07 mW/cm<sup>2</sup> in the case of metal wires with 50-nm-thick Cr/250-nm-thick Al layers formed on TaO<sub>x</sub> layers over air vacancies. However, the lower detection limit was 2 mW/cm<sup>2</sup> in the case of the metal wires formed directly on quartz substrates. The low heat diffusivity of the air vacancy has an advantage in reducing heat diffusion from the metal sensors and thereby enhances their energy sensitivity.

### References

1. W.C. Tang, T.C. Nguyen, R.T. Howe: *Sens. Actuators*. Vol. B **20**, 25 (1989)
2. L. Lin, T.C. Nguyen, R.T. Howe, A.P. Pisano: *Proc. IEEE Micro Electro Mechanical Systems Workshop (MEMS-92)*, (Germany 1992) pp.226-231
3. C.H. Hsu, R.S. Muller: *IEEE Int. Conf. on Solid-State Sensors, Actuators (Transducers'91)*, San Francisco, 1991, pp. 659-662
4. J. Bernstein, S. Cho, A.T. King, A. Kourepenis, P. Maciel, M. Weinberg: *Proc. IEEE Micro Electro Mechanical Systems Workshop (MEMS-93)*, Ft. Lauderdale, 1993, pp. 143-148
5. Y.H. Cho, B.M. Kwak, A.P. Pisano, R.T. Howe: *Proc. IEEE Micro Electro Mechanical Systems Workshop (MEMS-93)*, Ft. Lauderdale, 1993, pp. 93-98
6. R. Meyer: *IEDM Tech.Dig.* 197 (1991)
7. T. Kaeriyama: *OYO BUTURI* **68**, 285 (1999)
8. M.B. Anand, M. Yamada, H. Shibata: *IEEE Trans. Electron Devices* **44**, 1965 (1997)
9. N. Hacker: *MRS Bulletin (Materials Research Society, Pittsburg 1997)* p. 33
10. K. Endo, T. Tatsumi: *J. Appl. Phys.* **78**, 1370 (1995)
11. T. Aoki, Y. Shimizu, T. Kikkawa: *Extended Abstr. of MRS Spring Meet.*, O 1.8 (Materials Research Society, Pittsburg 1999)
12. E.S. Moyer, K. Chung, M. Spaulding, T. Deis, R. Boisvert, C. Saha, J. Bremmer: *Proc. Int. Interconnect Technology Conf. (New York 1999)* p. 196
13. B.A. Weinstein, G.J. Piermarini: *Phys. Rev. B* **12**, 1172 (1975)